HHS Public Access

Author manuscript

J Gene Med. Author manuscript; available in PMC 2018 March 01.

Published in final edited form as:

J Gene Med. 2017 March ; 19(3): . doi:10.1002/jgm.2942.

Humanized Chondroitinase ABC Sensitizes Glioblastoma Cells to Temozolomide

Alena Cristina Jaime-Ramirez[1], **Nina Dmitrieva**[1], **Ji Young Yoo**[1], **Yeshavanth Banasavadi-Siddegowda**[1], **Jianying Zhang**[2], **Theresa Relation**[3], **Chelsea Bolyard-Blessing**[1], **Jeffrey Wojton**[1], and **Balveen Kaur**[1]

[1]Department of Neurological Surgery, The Ohio State University Comprehensive Cancer Center, The James Cancer Hospital, and Solove Research Institute, Columbus, Ohio 43210, USA

[2]Center for Biostatistics Biomedical Informatics Department, The Ohio State University Comprehensive Cancer Center, The James Cancer Hospital, and Solove Research Institute, Columbus, Ohio 43210, USA

[3]Neuroscience Graduate Program, The Ohio State University Comprehensive Cancer Center, The James Cancer Hospital, and Solove Research Institute, Columbus, Ohio 43210, USA

Abstract

Introduction—Malignant gliomas (GBMs) are extremely aggressive and have a median survival of approximately 15 months. Current treatment modalities, which include surgical resection, radiation and chemotherapy, have done little to prolong the lives of GBM patients. Chondroitin sulfate proteoglycans (CSPG) are critical for cell-cell and cell-extra cellular matrix (ECM) interactions and are implicated in glioma growth and invasion. Chondroitinase (Chase) ABC is a bacterial enzyme that cleaves chondroitin sulfate disaccharide chains from CSPGs in the tumor ECM. Wild type Chase ABC has limited stability and/or activity in mammalian cells, therefore we created a mutant humanized version (Chase M) with enhanced function in mammalian cells.

Aims—We hypothesize that disruption of cell-cell and cell-ECM interactions by ChaseM and temozolomide will enhance chemotherapeutic availability and sensitivity of glioma cells.

Results—Utilizing primary patient derived neurospheres, we found that ChaseM decreases glioma neurosphere aggregation *in vitro*. Furthermore, an oncolytic HSV-1 virus expressing secreted ChaseM (OV-ChaseM) enhanced viral spread and glioma cell killing when compared to OV-Control, *in vitro*. OV-ChaseM plus TMZ combinatorial treatment resulted in a significant synergistic enhancement of glioma cell killing accompanied by an increase in apoptotic cell death. Intracellular flow cytometric analysis revealed a significant reduction in the phosphorylation of the pro-survival AKT protein following OV-ChaseM plus TMZ treatment. Lastly, in nude mice bearing intracranial GBM30 glioma xenografts, intratumoral OV-ChaseM plus TMZ (10 mg/kg by oral gavage) combination therapy resulted in a significant ($p<0.02$) enhancement of survival, when compared to each individual treatment alone.

[1]**Corresponding Author**: Balveen Kaur, PhD, Department of Neurological Surgery, 410 W. 12th Avenue, 385 Wiseman Hall, The Ohio State University, Columbus, OH 43210, Phone: (614) 292-5530 Fax: (614)688-4882 balveen.kaur@osumc.edu.

Disclosure of Potential Conflicts of Interest

No potential conflicts of interest were disclosed.

Conclusion—These data reveal that OV-ChaseM enhances glioma cell viral susceptibility and sensitivity to TMZ.

Keywords

Animal model; cancer-brain; chemotherapy; gene-delivery; HSV; oncolytic viruses; tumor-biology

Introduction

Malignant glioma, glioblastoma (GBM), is a very aggressive and common form of primary brain cancer in adults with a median survival of less than 15 months (1). Chondroitin sulfate proteoglycans (CSPGs), such as membrane-associated CSPG4/NG2, PTPRZ1 and CD44, and the lectican family members versican, aggrecan and brevican are frequently overexpressed in glioma and have been implicated in glioma cell growth, vascularization and invasion (2, 3). While several studies have demonstrated a functional role for the CS segments of CSPGs in glioma progression *in vitro* (4, 5), their significance in blocking the penetration of chemotherapeutics, such as temozolomide (TMZ), and/or role in promoting resistance has not been studied.

Chase ABC I (Chase) is a bacterial enzyme that depolymerizes a variety of CS glucosaminoglycan (GAG) chains, which are covalently attached to the CSPG core protein, without altering the core protein structure (6). Previous work from our laboratory indicated that degradation of the glioma ECM with an oncolytic virus (OV) expressing the Chase bacterial enzyme enhanced OV spread and anti-tumor efficacy both *in vitro* and *in vivo* (7, 8). The recent molecular characterization of Chase has revealed several potential glycosylation sites in the enzyme that can limit enzymatic function and/or /secretion in mammalian cells (9). Here, using site-directed mutagenesis of several potential glycosylation sites, we generated a humanized mutant Chase (ChaseM) enzyme that results in optimal enzymatic expression and function in mammalian cells. We have also generated an OV expressing the ChaseM enzyme and determined its effects on glioma cells in combination with TMZ. With the recent FDA approval of the T-Vec oncolytic HSV for non resectable melanoma, there is new hope for such novel treatment modalities for GBM patients (10, 11).

We hypothesize that disruption of cell-to-cell or cell-ECM interactions with a humanized Chondroitinase ABC (ChaseM) enzyme will enhance glioma cell chemotherapeutic availability and sensitivity. Utilizing patient derived neurospheres, we found that ChaseM decreases glioma neurosphere aggregation *in vitro*, akin to the phenotype observed with pharmacologic blockade of CSPG assembly. Oncolytic virus secreted ChaseM (OV-ChaseM) enhanced viral spread and glioma cell killing when compared to OV-Control, *in vitro*. Moreover, this enzymatic activity was maintained *in vivo*. In combination with TMZ, OV-ChaseM resulted in a significant and synergistic enhancement of glioma cell killing as compared to OV-Control plus TMZ and induced a significant reduction in the phosphorylation of the pro-survival AKT protein. *In vivo*, OV-ChaseM plus TMZ resulted in a significant increase in survival versus mice treated with TMZ or OV-ChaseM alone. Taken together, these data reveal that OV-ChaseM enhances glioma cell viral susceptibility and

sensitivity to TMZ and provide the rationale for novel treatment regiments to be implemented in the clinic.

Materials and Methods

Cells lines and reagents

Human glioma cells (U87ΔEGFR, LN229, Gli36ΔEGFR-H2B-RFP, U251) and Vero cells were cultured as previously described (7). Primary glioblastoma-derived cells (GB9, GB9-GFP, and GBM30) were generated at The Ohio State University or kindly provided by the Mayo Clinic (X12) and maintained in neurosphere cultures as described (7, 12). Cos-7 cells were purchased from the ATCC (Manassas, VA) and cultured accordingly. Cells were routinely monitored for morphology and growth changes. Chondroitinase ABC (Chase ABC), Methyl β-D-xylopyranoside and Temozolomide (TMZ) were obtained from Sigma-Aldrich (St. Louis, MO). Chondroitin sulfate A (CS A) was obtained from Seikagaku Biobusiness Corp (Japan). Mouse monoclonal anti CS-4 antibody (clone BE-123, Millipore, Temecula, CA) was used to probe for Chase functionality. Trypan blue exclusion using the Cell Countess (Life Technologies, Inc. Carlsbad, CA) was used to determine glioma cell proliferation.

ChaseM generation and viruses

Cloning and construction of wild type Chase ABC has been described earlier (7). Primers G1, G2, G3 and G5, described in (9), were used to mutate the selected N-glycosylation sites of Chondroitinase ABC I cDNA using the QuickChange Lightning Multi Site-Directed Mutagenesis Kit (Agilent Technologies, La Jolla, CA. Mutant Chase ABC cDNA was utilized to generate OV-ChaseM viruses as previously described (7). OV-Control was generated without any Chase insertion.

Tests for secretion of active Chase ABCI *in vitro* and *in vivo*

To determine Chase ABC *in vitro* activity, Cos-7 cells were transfected with pcDNA3.1 ChaseN or ChaseM plasmids using the FuGENE 6 transfection reagent (Roche Applied Science Inc, Indianapolis, IN). After 24 hours, U87ΔEGFR concentrated medium (source of CSPGs) was added to the Cos-7 transfected cells. Forty eight hours later the medium from Cos-7 cells was collected, concentrated analyzed via Western Blot analysis using the BE-123 antibody, which recognizes the CS stubs left behind after CSPG digestion by the Chase ABC enzyme (7). To assess Chase ABC activity *in vivo*, GB9-GFP positive glioma cells were electoporated with 5 ug of pcDNA3.1 LacZ or ChaseM using the Amaxa Mouse Neural Stem Cell Nucleofector Kit (Lonza, Walkersville, MD). These cells were then injected into the striatum of athymic nude mice as previously described (300,000 cells/mouse and 3 mice for each condition) (7). Seven days post implantation, tumors were harvested, fixed in 4%PFA, and assayed for BE-123 reactivity (7).

Aggregation and assays

U87ΔEGFR, Gli36 ΔEGFR, U251cells were plated as single cells in 6-well or 24-well Ultra low attachment plates (Corning, NY) with DMEM medium supplemented with 2%FBS or neurosphere medium. Cells were then incubated in a 37°C shaking incubator for 48 hours in

the presence of 0.015 U/ml of Chase ABC or 5 uM methyl β- D- xylopyranoside, which was replenished every 24 hours. CS A (0.2 μg/μl) were added to U87ΔEGFR cells for 48 hours and cell aggregation was monitored using a Nikon Eclipse TE2000-U fluorescent microscope. Images were taken from 4-10 representative view fields, and the aggregates/ neurosphere diameters were measured using Image J software to calculate the area. GBM30 or X12 glioma cells were transfected with ChaseN, ChaseM, or control plasmid (5 μg) using the Amaxa Mouse Neural Stem Cell Nucleofector Kit (Lonza, Walkersville, MD) as directed or infected with OV-Control, OV-ChaseN or OV-ChaseM at an MOI of 0.005 and seeded into 96-well plates in triplicate to assesses the effects of Chase ABC on neurosphere culture following 72 hrs of culture via light microscopy.

Flow cytometric analysis

All flow cytometric analyses were conducted using a Becton Dickinson fluorescence-activated cell sorter (FACS) LSRII (Becton-Dickinson, San Jose, CA) and analyzed using the FlowJo Software (Ashland, OR) as previously described (13). Oncolytic viral GFP was assessed using X12 glioma cells that were treated at various multiplicity of infection (MOI) and collected five days post infection. Cells were then fixed in 1% formalin and the percentage of GFP positive cells was determined. Twenty-four hours post OV infection glioma cells were treated with TMZ and collected five days later. The percentage of dead cells was then quantified using a Live/Dead Fixable Dead cell stain kit (Invitrogen, Carlsbad, CA) per the manufacturer's instructions. Cellular apoptosis was determined using Annexin V-V450 and 7AAD (BD Biosciences Pharmingen, San Diego, CA) in accordance with the manufacturer. Intracellular pAKTSer473-BV421 staining (BD Biosciences Pharmingen, San Diego, CA) was performed as indicated by the manufacturer. The mean fluorescence intensity (MFI) was calculated by taking the area under the curve for pAKT stained samples after subtraction of the area under the curve for the respective isotype stained control for each treatment group.

Animal studies

All murine studies were housed and handled in accordance with the Subcommittee on Research Animal Care guidelines at the Ohio State University and were approved by the Institutional Review Board. For all intracranial tumor studies, 6-8 week old athymic nu/nu mice (Target Validation Shared Resource, The Ohio State University) were anesthetized and fixed into a stereotactic apparatus. A burr hole was then drilled at 2 mm lateral to bregma to a depth of 3 mm, as previously described (7). For GBM30 experiments, n=5 athymic nude mice were implanted with 100,000 tumor cells and then treated with 3×10^5 pfu of OV-ChaseM seven days post implantation. Mice were treated with 10 mg/kg of TMZ on days 8-12 via oral gavage post tumor implant. Animals were observed daily and were euthanized when they displayed symptoms of tumor burden, such as weight loss and/or hunched posture. Animal experiments were performed in duplicate.

Statistical analysis

The GraphPad Prism 6 (GraphPad Software, Inc, La Jolla, CA), R3.3.1 (R Foundation for Statistical Computing, Vienna, Austria) and SAS 9.3 (SAS Institute, Cary, NC) were used for statistical analysis. For continuous measurement following normal distribution, such as

cellular proliferation and aggregation, a two-sample *t* test was used to compare two independent conditions. A one-way ANOVA model was used to compare three or more conditions. A two-way ANOVA model was used for interaction contrast or synergistic effect tests. For survival data, survival functions were estimated by the Kaplan-Meier method and were compared among the groups by the log-rank test. The *p* value was adjusted for multiple comparisons by Holm's procedure. A *p* value of 0.05 or less was considered statistically significant.

Results

Chondroitinase ABCI decreases neurosphere formation in glioma cell lines and patient-derived neurospheres

To evaluate the impact of removal of CSPG in glioma ECM we measured the ability of glioma neurospheres (NS) to form neurospheres. Treatment of glioma cultures with purified Chase ABC revealed a striking decrease in glioma cell aggregation, (**Fig. 1A**). Quantification of the size of area covered by the neurospheres from representative microscopic images indicated that the removal of CS GAGs significantly reduced the ability of glioma cells to form clusters (±95%CI, $p<0.0001$ for each cell line tested) (**Fig. 1B**). Interestingly the smaller neurospheres were not accompanied by a reduction in the number of NS formed, or the viability of treated cells suggesting that Chase ABC treatment had an impact on cell-cell aggregation without affecting self-renewal or the proliferation of glioma cells (**Fig. 1C**). Chase ABC treatment digests the CS proteoglycans on secreted/membrane bound CSPG, releasing CS disaccharides in the ECM. To evaluate if the reduced NS aggregation observed after Chase ABC treatment was due to reduced CSPG or released CS disaccharides we evaluated the effect of treating glioma NS cultures with β-D-xylopyranoside (XP), to reduce CSPG glycosylation/secretion from cells or treatment with exogenous CS chains to mimic the released end product after treatment of CSPG with chase ABC (14-16). Briefly three different glioma cell lines (Gli36ΔEGFR, U251 and U87ΔEGFR) grown in a three dimensional cell culture were incubated with β-D-xylopyranoside to reduce CSPG glycosylation (17, 18). Forty-eight hours post treatment, a moderate decrease in glioma sphere aggregation was observed in cells treated with β-D-xylopyranoside (**Fig. 1D**), suggesting a role for extracellular CSPG in glioma cell aggregation. To evaluate the contribution of CS disaccharides released after Chase treatment in inhibiting NS aggregates, we treated glioma cell derived neurospheres with CS or Chase, which resulted in a significant reduction of cell-cell adhesion, as determined by aggregation assays (**Fig. 1E and Supplementary Fig.1**). Collectively these results suggested that both the absence of CSPG as well as the presence of CS disaccharides released after Chase treatment inhibited NS aggregate formation. Thus CSPGs are critical for glioma cell-to-cell interactions and Chase treatment can significantly attenuate these glioma-glioma interactions and aggregation.

Generation of a Chase mutant (ChaseM) with enhanced functional secretion

Interestingly, transfection of a normal wild type Chase (Chase N) expressing plasmid into glioma NS cells did not show an obvious effect on glioma NS aggregation (**Fig. 2A**). The wild type bacterial Chase ABC enzyme has limited secretion/activity when expressed in

mammalian cells and mutation of potential glycosylation sites within the catalytic domain of the bacterial sequence has been demonstrated to increase enzymatic activity (9). Therefore, we engineered a mutant, humanized form of the Chase enzyme (ChaseM) that was mutated for five potential N-glycosylation sites (N282Q, N338Q, N345Q, S517Q, and N675Q) shown to interfere with its function due to glycosylations upon expression in mammalian cells (9), (**Table 1**). NS cells transfected with ChaseM revealed reduced NS aggregation as compared to control or WT Chase transfected cells (**Fig. 2A**). Furthermore, the *in vitro* enzymatic activity of the Chase enzyme was also confirmed via staining for immunoreactive CS stubs using the BE123 antibody. Here, Cos-7 cells were first transfected with pcDNA3.1 ChaseN or ChaseM plasmids. Concentrated U87ΔEGFR (source of CSPGs) cell culture medium was then added to the transfected Cos-7 cells and for 48 hours, collected, concentrated and then subjected Western Blot analysis using the BE-123 antibody, which recognizes the stub left behind after CS digestion from CSPGs by Chase ABC (7). Presence of a smeared western blot lane revealed the presence of cleaved CS-stubs on the family of CSPG proteins and indicated the functionality of the secreted Chase enzyme (**Fig. 2B**). The *in vivo* activity of ChaseM was also confirmed using a glioma xenograft model. Briefly, GFP positive GB9-GFP tumor cells transfected with a control or ChaseM expressing plasmid were implanted into the striatum of athymic mice as previously described [9]. Seven days post tumor implant, mice were euthanized and brains were analyzed for CS stubs indicative of Chase ABC activity. Immunohistochemistry using the BE123 antibody identified areas of CSPG digestion in the tumor ECM in GBM30 cells transfected with ChaseM (**Fig. 2C**). Importantly, ChaseM secretion into the tumor ECM did not enhance glioma cell invasion in vivo (data not shown). These results indicate that the ChaseM enzyme was secreted in its active form by transfected mammalian cells both *in vitro* and *in vivo* without enhancing glioma cell invasion.

Oncolytic virus (OV) with a functional ChaseM enzyme enhances viral spread and glioma cell killing

We have previously described the ability of Chase to enhance OV spread in glioma neurospheres (7). To determine if the humanization of ChaseM could enhance the anti-glioma efficacy of a herpes simplex I (HSV-1) OV we generated a novel ChaseM expressing OV (OV-ChaseM) (**Supplemental Fig. 2**) (7). Primary GBM neurosphere derived cells were infected with the indicated virus and allowed to form aggregates over 72 hours. Analysis of aggregate size of infected GBM30 (**Fig. 3A**) and X12 (**Fig. 3B**) glioma cells revealed a significant inhibition of glioma cell aggregation after OV-Chase M infection relative to control and wild-type normal Chase (Chase N) expressing OV ($p<0.001$) (**Fig. 3A-B**). Since only the humanized mutant Chase OV showed a significant reduction in the ability of GBM neurospheres to form aggregates, we then tested the ability of this mutant to enhance the oncolytic killing of glioma cells alone and/or with chemotherapy.

To evaluate if the ChaseM virus resulted in increased spread and infection of glioma NS, the indicated neurosphere cultures were treated with either OV-Control or OV-ChaseM and then evaluated for infection. Flow cytometry for GFP positive infected cells revealed better virus infection resulting in an increased number of infected cells in neurospheres treated with OV-ChaseM as compared to OV-Control five days post infection (**Fig. 3C**). Next, to examine the

oncolytic ability of OV-ChaseM, X12 patient derived neurospheres were infected at an MOI of 0.005 for five days and cells were then harvested and assayed for cell killing after live/dead cell staining (Invitrogen) via flow cytometric analysis. Representative live/dead histograms reveal an obvious induction of glioma cell death following OV treatment (**Fig. 3D**). At every MOI tested (0.0025, 0.005 and 0.01), OV-ChaseM resulted in a significant enhancement of glioma cell killing when compared to OV-Control or untreated cells ($p<0.05$) (**Fig. 3E**). Taken together, these data reveal that OV-ChaseM contains a functional ChaseM enzyme and enhances viral replication and glioma cell killing *in vitro*.

OV-ChaseM enhances temozolomide (TMZ) induced apoptotic cell killing of glioma neurospheres

Since a diminished capacity to form aggregates implied a decreased physical barrier for the spread of chemotherapeutic drugs (7, 18, 19), we postulated that ChaseABC would be an effective therapeutic modality when combined with chemotherapy. The ability of OV-ChaseM in combination with Temozolomide (TMZ) to induce apoptosis was assessed using Annexin V/7-AAD (BD) and live/dead staining (Invitrogen) via flow cytometric analysis. Here, glioma cells were treated with OV one day prior to TMZ and collected for analysis five days thereafter. There was a significant increase in AnnexinV/7AAD dual positive apoptotic glioma cells following OV-ChaseM plus TMZ treatment, indicative of apoptotic cell death, when compared to all other treatment groups ($p<0.0001$) (**Fig. 4A**). Additionally, specific examination of glioma cell death using a live/dead cell stain also revealed a significant induction of cell death following OV-ChaseM plus TMZ treatment ($p<0.0001$) (**Fig. 4B**). Using a two-way ANOVA model to test for synergistic interactions, we determined that there was a significant and synergistic interaction between OV-ChaseM and TMZ that resulted in the induction of glioma cell death ($p<0.002$). Taken together, these data indicate the induction of apoptosis observed following TMZ treatment is significantly enhanced by OV infection, with maximal sensitivity observed using an OV expressing the ChaseM enzyme.

OV-ChaseM plus TMZ inhibits pro-survival AKT responses in glioma neurospheres

The marked increase in glioma neurosphere apoptosis and cell death led us to further interrogate the cellular signaling alterations that occur following OV-ChaseM plus TMZ treatment. AKT, a serine/threonine kinase that is central to the RTK/PTEN/PI3K pathway, plays a critical role in cancer cell growth and survival (20). Moreover, AKT activation, via phosphorylation at Serine473, is associated with TMZ chemoresistance in glioblastoma cells (21). Therefore, we next examined whether or not OV-ChaseM sensitized glioma neurospheres to TMZ by affecting this crucial cell signaling hub. X12 primary patient-derived glioma neurospheres were infected with OV-Control or OV-ChaseM for 24 hrs prior to TMZ treatment for 5 days. Glioma cells were then harvested and assayed for intracellular pAKTSer473 via flow cytometric analysis. HSV-1 encoded miR H6 has been shown to increase intracellular AKT phosphorylation (22). Consistent with this, we observed increased AKT phosphorylation in response to oncolytic virus infection with OV-Control or OV-ChaseM. Interestingly, TMZ treatment alone had no effect on pAKT levels when compared to untreated cells (**Fig. 4C**). Surprisingly, there was a significant and synergistic interaction between OV-ChaseM and TMZ treatment in the reduction of the number of

pAKT positive cells (**Fig. 4C**: 21.9% relative to 61.9% and 61.1% for OV-ChaseM + TMZ, OV-ChaseM and TMZ alone, respectively) and the total levels of phosphorylated AKTSer473, as measured by mean fluorescence intensity (MFI), when compared to all other treatment groups ($p<0.0001$) (**Fig. 4D**). Individual MFI values are listed in the inset boxes of **Fig. 4C** and the mean from three independent experiments normalized to untreated cells is quantified if **Fig. 4D**. Moreover, there was a significant synergistic interaction of OV-ChaseM and TMZ in the reduction of pAKT levels ($p<0.008$). This pAKT inhibition mediated by combinatorial therapy indicated that OV-ChaseM infection sensitized glioma neurospheres to TMZ, making them more susceptible to its chemotherapeutic, anticancer effects.

OV-ChaseM plus TMZ combinatorial therapy enhances survival *in vivo*

Next, we tested the therapeutic efficacy of combining OV-ChaseM with TMZ in mice bearing intracranial tumors. Athymic nude mice bearing intracranial GBM30 tumors were treated with 3×10^5 pfu of OV-ChaseM via intratumoral injection as previously described (7). Following OV infection, mice were treated with 10 mg/kg of TMZ for five days via oral gavage. Here, mice treated with TMZ exhibited a significant survival advantage when compared to saline treated mice (**Fig. 5**) ($p=0.05$). Interestingly, OV-ChaseM plus 10 mg/kg TMZ combination therapy resulted in a significant enhancement of murine survival, when compared to all other individual treatment groups ($p<0.02$). These data indicate the therapeutic efficacy of TMZ can be significantly improved following OV-ChaseM infection in an *in vivo* model of glioblastoma.

Discussion

The tumor microenvironment plays a critical role in the molecular pathways involved in glioma initiation, progression and metastasis. Extracellular matrix associated proteins, such as CSPGs are among these key players and are essential to the pro-tumorigenic cellular cascades involved in these processes. Elucidation of the mechanisms by which CSPGs drive tumorigenesis and metastasis may provide novel therapeutic approaches in cancer therapy (23). We have previously demonstrated that an OV-secreted Chase enzyme enhanced OV spread in glioma cells with enhanced *in vivo* efficacy (7). Based on these findings, we generated a second generation OV expressing a humanized Chase enzyme (ChaseM) that exhibited enhanced secretion and functionality in mammalian cells when compared to Chase. For the first time, using neurosphere models, we now demonstrate that CSPGs are directly involved in glioma cell-to-cell interactions. In this study, we found that the disruption of these ECM components resulted in diminished neurosphere aggregation without affecting cellular proliferation or viability. We also generated an OV expressing the humanized ChaseM enzyme, which resulted in enhanced virus replication and glioma cell killing, and a synergistic enhancement of the effects of TMZ. *In vivo*, OV-ChaseM plus TMZ combination therapy resulted in a significant survival advantage for glioma tumor-bearing mice when compared to each individual treatment.

Several CSPGs have previously been implicated in GBM tumorigenesis and metastasis. It is thought that they may be critical to glioma cell-to-cell or cell-to-ECM interactions or

adhesion in the tumor microenvironment. Importantly, CD44, versican, aggrecan, NG2 and PTPRZ1 have all been reported to be widely expressed in human GBMs (3). Studies conducted by Ulbricht *et al.* and Bourgonje *et al.*, also provide strong evidence for the ability of PTPRZ1 to drive glioma cell growth, migration and invasion *in vitro* and *in vivo* (24, 25). For example CS chain interactions in CD44 are known to be significant in the CD44 mediated cell-cell interactions (26), and their disruption has been shown to inhibit the growth of melanoma in mice (27-29). Similarly NG2 blocking antibodies led to a reduction in tumor growth and proliferation *in vivo*, as well as enhanced sensitivity to various chemotherapeutic agents (30-33). These studies highlight the importance and potential therapeutic targeting of CSPGs in cancer therapy. In our studies, a drastic reduction in glioma cell aggregation was observed following humanized ChaseM transfection and OV-ChaseM infection.

While the neurosphere formation to anti-cancer drugs is a strong prognostic indicator for the effectiveness of chemotherapy (19), *in vitro* treatment with Chase ABC did not affect glioma cell viability or proliferation implying that while CS chains on CSPG were important for aggregation, their removal did not affect glioma cell viability. Since cell-to-cell interactions have been implicated in resistance to chemotherapy and apoptosis (34), disruption of these interactions using OV-ChaseM enhanced glioma cell killing by TMZ. In corroboration with previous observations (35), we observed a significant and synergistic enhancement of glioma cell apoptotic cell killing, along with the marked reduction in AKT phosphorylation, a nodal point for pro-survival signal transduction of extracellular and intracellular oncogenic signals (36, 37). Our data as well as work from Kanai *et al.* (38) indicates that OV infection of glioma cells results in increased phosphorylation of AKT at Ser473. Cells treated with both TMZ and OV-ChaseM showed a significant and synergistic reduction in pAKT and increased glioma cell death.

Collectively our data demonstrate that OV-ChaseM infection allows for reduced glioma cell aggregation, thus enhancing TMZ penetration and inducing glioma neurosphere death via apoptosis. Furthermore, our *in vivo* findings illustrate a clear therapeutic advantage of combining OV-Chase with TMZ. Future studies will focus on elucidating a precise mechanism by which OV-ChaseM plus TMZ combination therapy, as well as other clinically relevant chemotherapeutic agents, enhance anti-tumor efficacy. The data provided from these studies could augment the therapeutic repertoire for glioblastoma patients and provide a novel OV to enhance anti-cancer drug distribution in solid tumors.

Supplementary Material

Refer to Web version on PubMed Central for supplementary material.

Acknowledgements

We would like to acknowledge the Analytical Cytometry Shared Resource, the Center for Biostatistics, and the Target Validation Shared Resources within the James Comprehensive Cancer Center, all at The Ohio State University.

Grant support: This work was supported by National Institutes of Health Grants R01 NS064607, P01 CA163205, R01 CA150153, and P30 CA016058 (BK), F32 (F32CA186542) (ACJR) and T32 CA009338 (CBB). Pelotonia Post Doctoral Fellowship (ACJR) and ACS grant IRG-67-003-50 (JYY).

References

1. Johnson DR, Leeper HE, Uhm JH. Glioblastoma survival in the United States improved after Food and Drug Administration approval of bevacizumab: a population-based analysis. Cancer. 2013; 119(19):3489–95. [PubMed: 23868553]
2. Viapiano MS, Matthews RT. From barriers to bridges: chondroitin sulfate proteoglycans in neuropathology. Trends Mol Med. 2006; 12(10):488–96. [PubMed: 16962376]
3. Wade A, Robinson AE, Engler JR, Petritsch C, James CD, Phillips JJ. Proteoglycans and their roles in brain cancer. FEBS J. 2013; 280(10):2399–417. [PubMed: 23281850]
4. Lobao-Soares B, Alvarez-Silva M, Mendes de Aguiar CB, Nicolau M, Trentin AG. Undersulfation of glycosaminoglycans induced by sodium chlorate treatment affects the progression of C6 rat glioma, in-vivo. Brain Res. 2007; 1131(1):29–36. [PubMed: 17174944]
5. Yang YL, Sun C, Wilhelm ME, Fox LJ, Zhu J, Kaufman LJ. Influence of chondroitin sulfate and hyaluronic acid on structure, mechanical properties, and glioma invasion of collagen I gels. Biomaterials. 2011; 32(31):7932–40. [PubMed: 21820735]
6. Afratis N, Gialeli C, Nikitovic D, Tsegenidis T, Karousou E, Theocharis AD, et al. Glycosaminoglycans: key players in cancer cell biology and treatment. FEBS J. 2012; 279(7):1177–97. [PubMed: 22333131]
7. Dmitrieva N, Yu L, Viapiano M, Cripe TP, Chiocca EA, Glorioso JC, et al. Chondroitinase ABC I-mediated enhancement of oncolytic virus spread and antitumor efficacy. Clin Cancer Res. 2011; 17(6):1362–72. [PubMed: 21177410]
8. Kaur B, Chiocca EA, Cripe TP. Oncolytic HSV-1 virotherapy: clinical experience and opportunities for progress. Curr Pharm Biotechnol. 2012; 13(9):1842–51. [PubMed: 21740359]
9. Muir EM, Fyfe I, Gardiner S, Li L, Warren P, Fawcett JW, et al. Modification of N-glycosylation sites allows secretion of bacterial chondroitinase ABC from mammalian cells. J Biotechnol. 2010; 145(2):103–10. [PubMed: 19900493]
10. Andtbacka RH, Kaufman HL, Collichio F, Amatruda T, Senzer N, Chesney J, et al. Talimogene Laherparepvec Improves Durable Response Rate in Patients With Advanced Melanoma. J Clin Oncol. 2015; 33(25):2780–8. [PubMed: 26014293]
11. Killock D. Skin cancer: T-VEC oncolytic viral therapy shows promise in melanoma. Nat Rev Clin Oncol. 2015; 12(8):438. [PubMed: 26077044]
12. Hu B, Nandhu MS, Sim H, Agudelo-Garcia PA, Saldivar JC, Dolan CE, et al. Fibulin-3 promotes glioma growth and resistance through a novel paracrine regulation of Notch signaling. Cancer Res. 2012; 72(15):3873–85. [PubMed: 22665268]
13. Yoo JY, Jaime-Ramirez AC, Bolyard C, Dai H, Nallanagulagari T, Wojton J, et al. Bortezomib treatment sensitizes oncolytic HSV-1 treated tumors to NK cell immunotherapy. Clin Cancer Res. 2016
14. Denholm EM, Lin YQ, Silver PJ. Anti-tumor activities of chondroitinase AC and chondroitinase B: inhibition of angiogenesis, proliferation and invasion. Eur J Pharmacol. 2001; 416(3):213–21. [PubMed: 11290371]
15. Fthenou E, Zong F, Zafiropoulos A, Dobra K, Hjerpe A, Tzanakakis GN. Chondroitin sulfate A regulates fibrosarcoma cell adhesion, motility and migration through JNK and tyrosine kinase signaling pathways. In Vivo. 2009; 23(1):69–76. [PubMed: 19368127]
16. Haylock-Jacobs S, Keough MB, Lau L, Yong VW. Chondroitin sulphate proteoglycans: extracellular matrix proteins that regulate immunity of the central nervous system. Autoimmun Rev. 2011; 10(12):766–72. [PubMed: 21664302]
17. Hazlehurst LA, Landowski TH, Dalton WS. Role of the tumor microenvironment in mediating de novo resistance to drugs and physiological mediators of cell death. Oncogene. 2003; 22(47):7396–402. [PubMed: 14576847]

18. Westhoff MA, Zhou S, Bachem MG, Debatin KM, Fulda S. Identification of a novel switch in the dominant forms of cell adhesion-mediated drug resistance in glioblastoma cells. Oncogene. 2008; 27(39):5169–81. [PubMed: 18469856]
19. Mihaliak AM, Gilbert CA, Li L, Daou MC, Moser RP, Reeves A, et al. Clinically relevant doses of chemotherapy agents reversibly block formation of glioblastoma neurospheres. Cancer Lett. 2010; 296(2):168–77. [PubMed: 20435409]
20. Engelman JA. Targeting PI3K signalling in cancer: opportunities, challenges and limitations. Nat Rev Cancer. 2009; 9(8):550–62. [PubMed: 19629070]
21. Wu L, Yang L, Xiong Y, Guo H, Shen X, Cheng Z, et al. Annexin A5 promotes invasion and chemoresistance to temozolomide in glioblastoma multiforme cells. Tumour Biol. 2014; 35(12): 12327–37. [PubMed: 25245332]
22. Zhao H, Zhang C, Hou G, Song J. MicroRNA-H4-5p encoded by HSV-1 latency-associated transcript promotes cell proliferation, invasion and cell cycle progression via p16-mediated PI3K-Akt signaling pathway in SHSY5Y cells. Int J Clin Exp Med. 2015; 8(5):7526–34. [PubMed: 26221296]
23. Asimakopoulou AP, Theocharis AD, Tzanakakis GN, Karamanos NK. The biological role of chondroitin sulfate in cancer and chondroitin-based anticancer agents. In Vivo. 2008; 22(3):385–9. [PubMed: 18610752]
24. Bourgonje AM, Navis AC, Schepens JT, Verrijp K, Hovestad L, Hilhorst R, et al. Intracellular and extracellular domains of protein tyrosine phosphatase PTPRZ-B differentially regulate glioma cell growth and motility. Oncotarget. 2014; 5(18):8690–702. [PubMed: 25238264]
25. Ulbricht U, Eckerich C, Fillbrandt R, Westphal M, Lamszus K. RNA interference targeting protein tyrosine phosphatase ζ/receptor-type protein tyrosine phosphatase β suppresses glioblastoma growth in vitro and in vivo. Journal of Neurochemistry. 2006; 98:1497–506. [PubMed: 16923162]
26. Hayes GM, Chiu R, Carpenito C, Dougherty ST, Dougherty GJ. Identification of sequence motifs responsible for the adhesive interaction between exon v10-containing CD44 isoforms. J Biol Chem. 2002; 277(52):50529–34. [PubMed: 12407110]
27. Theocharis AD, Skandalis SS, Tzanakakis GN, Karamanos NK. Proteoglycans in health and disease: novel roles for proteoglycans in malignancy and their pharmacological targeting. FEBS J. 2010; 277(19):3904–23. [PubMed: 20840587]
28. Wu YJ, La Pierre DP, Wu J, Yee AJ, Yang BB. The interaction of versican with its binding partners. Cell Res. 2005; 15(7):483–94. [PubMed: 16045811]
29. Zeng C, Toole BP, Kinney SD, Kuo JW, Stamenkovic I. Inhibition of tumor growth in vivo by hyaluronan oligomers. Int J Cancer. 1998; 77(3):396–401. [PubMed: 9663602]
30. Chekenya M, Krakstad C, Svendsen A, Netland IA, Staalesen V, Tysnes BB, et al. The progenitor cell marker NG2/MPG promotes chemoresistance by activation of integrin-dependent PI3K/Akt signaling. Oncogene. 2008; 27(39):5182–94. [PubMed: 18469852]
31. Kmiecik J, Gras Navarro A, Poli A, Planaguma JP, Zimmer J, Chekenya M. Combining NK cells and mAb9.2.27 to combat NG2-dependent and anti-inflammatory signals in glioblastoma. Oncoimmunology. 2014; 3(1):e27185. [PubMed: 24575382]
32. Poli A, Wang J, Domingues O, Planaguma J, Yan T, Rygh CB, et al. Targeting glioblastoma with NK cells and mAb against NG2/CSPG4 prolongs animal survival. Oncotarget. 2013; 4(9):1527–46. [PubMed: 24127551]
33. Wang J, Svendsen A, Kmiecik J, Immervoll H, Skaftnesmo KO, Planaguma J, et al. Targeting the NG2/CSPG4 proteoglycan retards tumour growth and angiogenesis in preclinical models of GBM and melanoma. PLoS One. 2011; 6(7):e23062. [PubMed: 21829586]
34. Santini MT, Rainaldi G, Indovina PL. Apoptosis, cell adhesion and the extracellular matrix in the three-dimensional growth of multicellular tumor spheroids. Crit Rev Oncol Hematol. 2000; 36(2-3):75–87. [PubMed: 11033298]
35. Kanai R, Rabkin SD, Yip S, Sgubin D, Zaupa CM, Hirose Y, et al. Oncolytic virus-mediated manipulation of DNA damage responses: synergy with chemotherapy in killing glioblastoma stem cells. J Natl Cancer Inst. 2012; 104(1):42–55. [PubMed: 22173583]
36. Cheng JQ, Lindsley CW, Cheng GZ, Yang H, Nicosia SV. The Akt/PKB pathway: molecular target for cancer drug discovery. Oncogene. 2005; 24(50):7482–92. [PubMed: 16288295]

37. Parsons DW, Jones S, Zhang X, Lin JC, Leary RJ, Angenendt P, et al. An integrated genomic analysis of human glioblastoma multiforme. Science. 2008; 321(5897):1807–12. [PubMed: 18772396]

38. Kanai R, Wakimoto H, Martuza RL, Rabkin SD. A novel oncolytic herpes simplex virus that synergizes with phosphoinositide 3-kinase/Akt pathway inhibitors to target glioblastoma stem cells. Clin Cancer Res. 2011; 17(11):3686–96. [PubMed: 21505062]

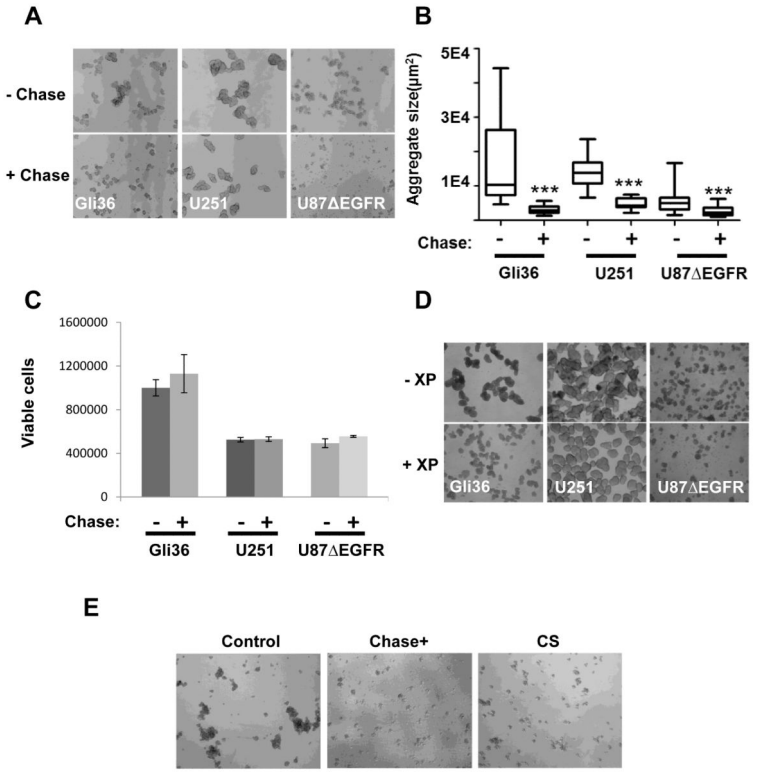

Figure 1. CSPG cleavage attenuates glioma cell aggregation. A

The indicated glioma cells were treated with or without 0.015 U/mL of the purified Chondroitinase ABCI (Chase) enzyme in low adherence plates. The ability of treated versus untreated cells to form neurospheres was assessed 48 hrs post treatment. Data shown are representative images of aggregrates formed from untreated (upper panels) and Chase treated (lower panels) cultures. **B.** Data shown are mean aggregate sizes (±95%CI) from cultures treated with or without Chase (***$p<0.0001$ for each cell line tested when compared to untreated cultures) quantified from at least 6 view fields per well and n=3 wells per condition. **C.** Data shown are the mean (± 95%CI) of cellular viability of glioma cell aggregates treated with or without Chase, as measured by Trypan Blue exclusion with n=3 wells per treatment condition ($p=0.38$; and $p=0.096$; and $p=0.82$ for Gli36, U251 and U87ΔEGFR, respectively). **D.** The indicated glioma cells were treated with 5μM β-D-xylopyranoside (XP, an inhibitor of CS glycosylation) for 48 hrs (replenished every 24 hrs). Glioma cell aggregation was then observed. Light microscopic images of glioma cell aggregates in untreated (upper panels) and treated cultures (bottom panels). **E.** U87ΔEGFR glioma cells were cultured in 24-well low adherence plates (50000 cells per well, n=3 wells per treatment condition) for 24 hrs following treatment with 0.015 U/mL of the purified Chase enzyme or 0.2 ug/mL of purified CS. Representative images of glioma cell aggregates under light microscopy following treatment. All experiments were performed in triplicate with at least three independent replicates.

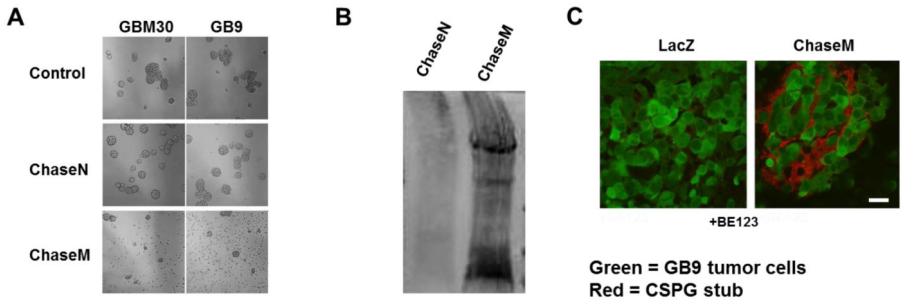

Figure 2. Creation of mutant Chondroitinase ABCI (ChaseM) with enhanced functional activity.

A Representative images of the indicated glioma cells transfected with plasmid encoding for beta galactosidase (control), wild type normal Chase (Chase N) or humanized mutant Chase (Chase M). **B.** Cos-7 mammalian cells were transfected with plasmids encoding for ChaseN (unmodified Chase DNA) or ChaseM (Mutant Chase) then cultured with concentrated medium from U87ΔEGFR glioma cells (the source of CSPGs) for 48 hrs. Cos-7 cell culture medium was then concentrated and subjected to CS stub Western Blot analysis using the BE123 antibody clone. Immunoreactivity is indicative of Chase enzymatic cleavage activity. **C.** Immunofluorescent images of tumor bearing brain sections from mice implanted with Green fluorescent protein (GFP) positive GB9 tumor cells (indicated in green) transiently transfected with a pcDNA3.1 LacZ control or pcDNA3.1 ChaseM plasmids and stained with the BE123 CS stub recognition antibody (CSPG cleavage staining indicated in red). Scale bar = 100μm. All *in vitro* and *in vivo* experiments were performed using an $n \geq 3$ triplicate in at least three independent replicates.

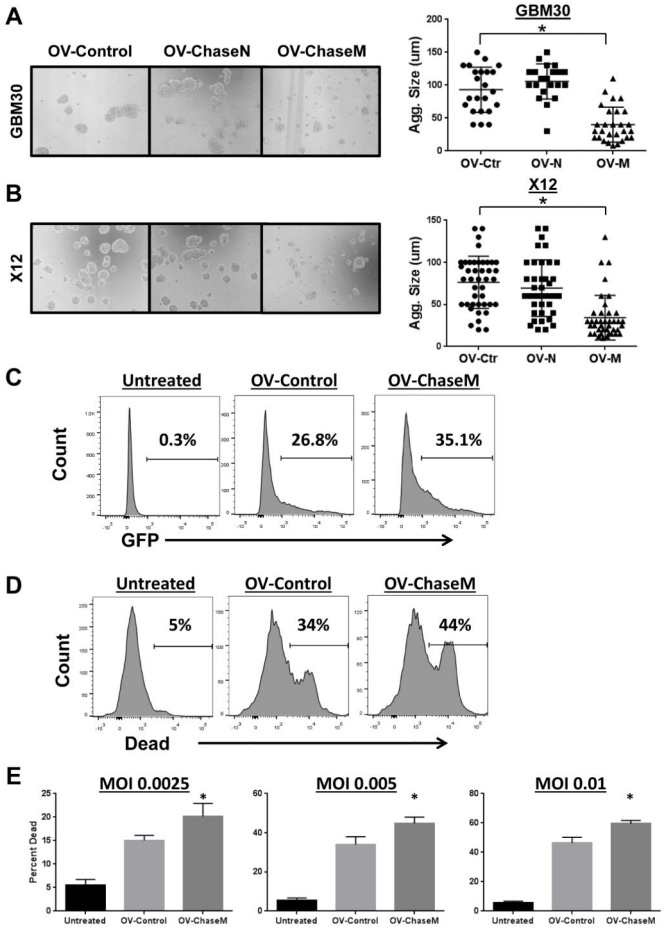

Figure 3. OV-ChaseM enhances viral spread and glioma cell killing. A-B

Representative 10X magnification light microscopy images for the GBM30 (**A**) and X12 (**B**) glioma cell aggregates infected with OV-Control (OV-Ctr), OV-ChaseN (OV-N) or OV-ChaseM (OV-M) (MOI of 0.005), 72 hrs post infection. Quantification of individual aggregate sizes (Agg. Size) in random view fields per cell line is indicated to the right. **C.** Histograms of GFP positive X12 neurospheres (MOI 0.005) five days post infection as determined by flow cytometric analysis using a BD LSR II. **D.** Representative histograms of dead cells obtained from flow cytometric analysis (using live and dead cell staining; Invitrogen) to determine the killing capacity of OV-ChaseM versus OV-Control. **E.** Quantification of the percentage of dead cells at various MOIs is indicated. *indicates OV-ChaseM difference when compared to all other treatment groups with $p<0.05$. All experiments were performed in triplicate with at least three independent replicates.

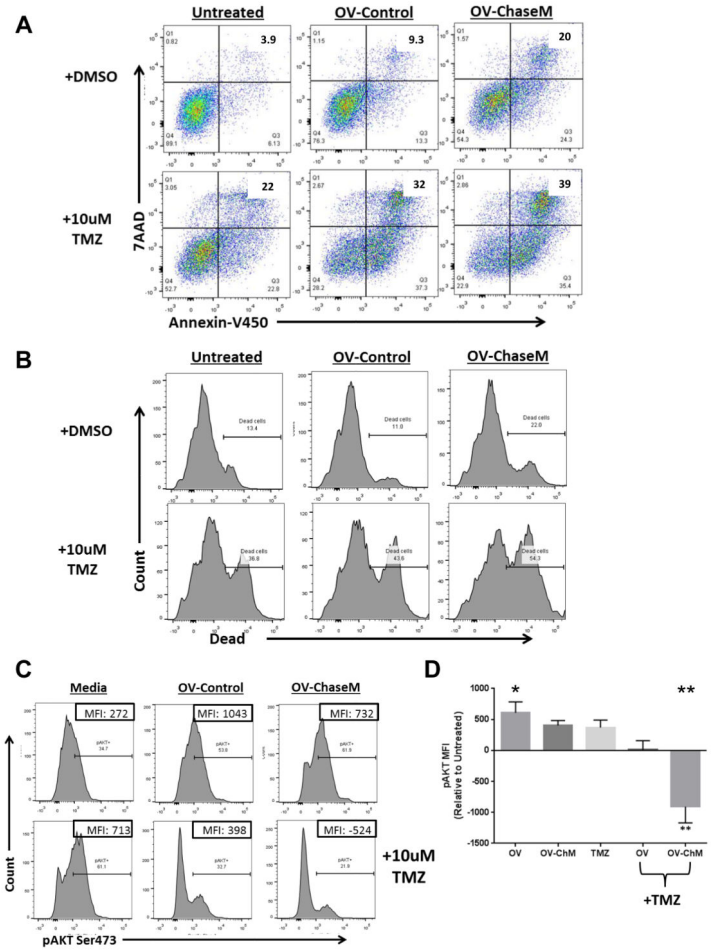

Figure 4. TMZ induced glioma cell apoptotic cell killing is enhanced with OV-ChaseM *in vitro*

X12 primary patient-derived glioma neurospheres were infected at an MOI of 0.005 for 24 hrs prior to treatment with 10uM of TMZ for 5 days. Following treatment, glioma neuropheres were dissociated and stained as indicated **A.** Representative Annexin V/7AAD scatter plot analysis of cells. The number in each quadrant reflects the percentage of events in that quadrant. **B.** Representative histograms of live/dead cell populations for cells treated as indicated. **C.** Representative histograms of intracellular pAKT (anti-pAKTSer473-BV421) for each treatment group. Percent of cells staining positive for pAKT is indicated above the bars in each histogram. Numbers in inset boxes represent the mean fluorescence intensity (MFI) calculated as the area under the curve after pAKT staining (corrected for the isotype stained baseline) for each treatment group. **D.** Quantification of the MFI for intracellular pAKTSer473 obtained from each treatment group, corrected for the MFI of untreated cells (n=3/group). *indicates OV-Control difference when compared to untreated ($p<0.05$). ** indicates OV-ChaseM differences when compared to all other treatment groups ($p<0.0001$). All experiments were performed in triplicate with at least three independent replicates.

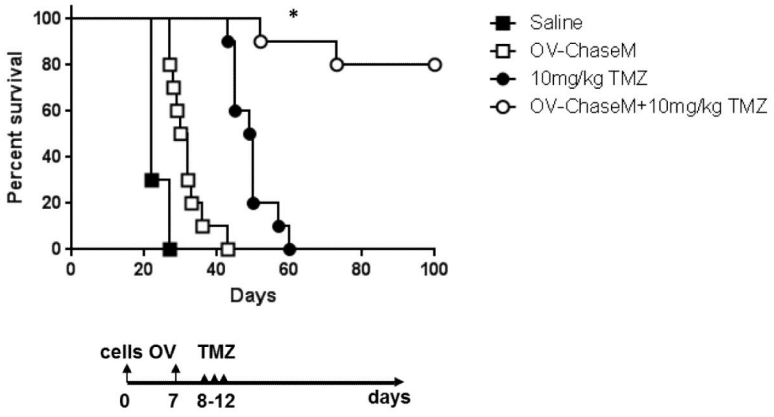

	Saline	OV-ChaseM	10mg/kg TMZ	OV-ChaseM+TMZ
Median survival	22	33	45	Undefined

Figure 5. OV-ChaseM plus TMZ combination therapy enhances murine survival

GBM30 glioma neurospheres were implanted into the striatum of athymic mice (n=10/group). Seven days post tumor implant, mice were treated with 3×10^5 pfu of OV-ChaseM via intratumoral injection and 10 mg/kg of TMZ via daily oral gavage on Days 8 through 12. Survival was assessed via Kaplan-Meir survival curves. *indicates OV-ChaseM+10 mg/kg TMZ differences when compared to all other treatment groups with $p<0.02$, n=10/group.

Table 1

List of Mutated amino acids created in mutant Chase ABC relative wild type Chase ABC. Mutation sites in the Chase enzyme engineered a mutant DNA to generate a humanized form of the Chase enzyme (ChaseM). The ChaseM sequence was preceded by a human IgG κ-chain leader sequence to enhance secretion and was five potential N-glycosylation sites were mutated (N282Q, N338Q, N345Q, S517Q, and N675Q).

Wild Type Chase	Mutant Chase
No Leader sequence	IgG κ secretion signal
282N	282Q
338N	338Q
345N	345Q
517N	517Q
675N	675Q